arXiv:1207.0168v1 [quant-ph] 1 Jul 2012

Complete hyperentangled-Bell-state analysis for photon systems assisted by quantum-dot spins in optical microcavities

Bao-Cang Ren, Hai-Rui Wei, Ming Hua, Tao Li, and Fu-Guo Deng*
Department of Physics, Applied Optics Beijing Area Major Laboratory,
Beijing Normal University, Beijing 100875, China

(Dated: July 3, 2012)

Bell-state analysis (BSA) is essential in quantum communication, but it is impossible to distinguish unambiguously the four Bell states in the polarization degree of freedom (DOF) of two-photon systems with only linear optical elements, except for the case in which the BSA is assisted with hyperentangled states, the simultaneous entanglement in more than one DOF. Here, we propose a scheme to distinguish completely the 16 hyperentangled Bell states in both the polarization and the spatial-mode DOFs of two-photon systems, by using the giant nonlinear optics in quantum dot-cavity systems. This scheme can be applied to increase the channel capacity of long-distance quantum communication based on hyperentanglement, such as entanglement swapping, teleportation, and superdense coding. We use hyperentanglement swapping as an example to show the application of this HBSA.

PACS numbers: 03.67.Hk, 03.67.Mn, 42.50.Pq, 78.67.Hc

I. INTRODUCTION

Entanglement is the key quantum resource for quantum information processing and it plays a critical role in many important applications in quantum communication, such as quantum key distribution [1–5], quantum dense coding [6, 7], quantum teleportation [8], and entanglement swapping [9]. Some important goals in quantum communication require the complete and deterministic analysis of the Bell states. In 1999, Vaidman's [10] and L*ü*tkenhau's [11] groups put forward a Bell-state analysis (BSA) for teleportation with only linear optical elements. Unfortunately, with linear-optical elements, one can only obtain the optimal success probability of 50% both in theory [12] and in experiment [13–15]. The BSA on photon pairs entangled in one degree of freedom (DOF) attracted much attention [16–25].

The entanglement of photon pairs in several DOFs [26–30], called it hyperentanglement, is useful in quantum information processing, especially in quantum communication for completing BSA on polarizations of photon pairs [29–34], performing entanglement purification [35–40], distributing entangled polarization states faithfully [41], or improving the channel capacity. For example, Kwiat and Weinfurter [29] first introduced the way to distinguish the four orthogonal Bell states of photon pairs in the polarization DOF with the hyperentanglement in both the polarization DOF and the momentum DOF in 1998. In 2003, Walborn et al. [30] proposed a simple scheme for completing Bell-state measurement for photon pairs entangled in the polarization DOF or the momentum DOF by using hyperentangled states with linear optics. The experiments of a complete BSA have also been reported with polarization-time-bin hyperentanglement [31] and polarization-momentum hyperentanglement [32] later. It implies a complete BSA in the polarization DOF can be accomplished with hyperentanglement in a larger Hilbert space by introducing other DOFs. In 2008, Barreiro et al. [33] beat the channel capacity limit for linear photonic superdense coding with polarization-orbital-angular-momentum hyperentanglement. In 2002, Simon and Pan [35] proposed an entanglement purification protocol (EPP) using hyperentanglement in both the polarization and the spatial DOFs. In 2008, an efficient EPP based on a parametric down-conversion source was proposed, resorting to this hyperentanglement [36]. In 2010, deterministic EPPs were proposed with hyperentanglement [37–40]. In 2010, a faithful entanglement distribution scheme for polarization was proposed [41], resorting to the stability of the frequency entanglement of photon pairs.

Considering a large Hilbert space with an additional DOF, e.g., a quantum system in a hyperentangled state in two DOFs which span the Hilbert space with 16 orthogonal Bell states, one can not distinguish them completely with only linear optics. In 2007, Wei et al. [34] pointed out that 7 states in the group of 16 orthogonal Bell states is distinguishable with only linear optics. If non-linear optics is introduced, these 16 orthogonal Bell states can be distinguished completely. In 2010, Sheng et al. [42] presented a complete hyperentangled BSA (HBSA) with cross-Kerr nonlinearity. Although a lot of works have been studied on cross-Kerr nonlinearity [43], a clean cross-Kerr nonlinearity in the optical single-photon regime is still quite a controversial assumption with current technology [44, 45]. In recent years, a solid state system based on an electron spin in a quantum dot (QD) has attracted much attention with its giant nonlinearity. In 2008, Hu et al. [46] proposed a quantum nondemolition method using the interaction of left-circular and right-circular polarized lights with one-side QD-cavity system. This nonlinear optics in one-side QD-cavity system can

---

*Corresponding author. Email address: fgdeng@bnu.edu.cn

be used to construct multi-photon entangler [46, 47] and photonic polarization BSA [48].

In this article, we present complete HBSA with the nonlinear optics based on one-side QD-cavity system. It can be used to distinguish completely the 16 hyperentangled Bell states in both the polarization and the spatial-mode DOFs of two-photon systems. This scheme divides the process for HBSA into two steps. The first step is to distinguish the four Bell states in spatial-mode DOF, without destroying the two-photon system itself and its state in the polarization DOF. This task should resort to quantum nondemolition detectors (QNDs) based on one-side QD-cavity system. In the second step, one can adjust the QD-cavity systems to distinguish the four Bell states in the polarization DOF. This HBSA scheme can be applied to increase the channel capacity of long-distance quantum communication based on hyperentanglement, such as entanglement swapping, teleportation, and superdense coding. We use hyperentanglement swapping as an example to show its application.

II. INTERACTION BETWEEN A CIRCULAR POLARIZED LIGHT AND A QD-CAVITY SYSTEM

Considering a singly charged QD in a cavity, e.g., a self-assembled In(Ga)As QD or a GaAs interface QD inside an optical resonant microcavity, the QD is located in the center of the cavity to achieve a maximal light-matter coupling. With an excess electron injected into the QD, the singly charged QD shows the optical resonance with the negatively charged exciton X^- that consists of two electrons bound to one hole [49]. According to Pauli's exclusion principle, X^- has spin-dependent transitions [50]. If the excess electron in the QD is in the spin state $|\uparrow\rangle$, only the left circular polarized light $|L\rangle$ can be resonantly absorbed to create the negatively charged exciton in the state $|\uparrow\downarrow\Uparrow\rangle$ with two antiparallel electron spins. Here $|\Uparrow\rangle$ represents a heavy-hole spin state $|+\frac{3}{2}\rangle$. If the excess electron in the QD is in the spin state $|\downarrow\rangle$, only the right circular polarized light $|R\rangle$ can be resonantly absorbed to create the negatively charged exciton in the state $|\downarrow\uparrow\Downarrow\rangle$ with two antiparallel electron spins. Here $|\Downarrow\rangle$ represents the heavy-hole spin state $|-\frac{3}{2}\rangle$. They have different phase shifts when the photons in these two different circular polarized states are reflected from the QD-cavity system.

The whole process can be represented by Heisenberg equations for the cavity field operator $\hat{a}$ and X^- dipole operator σ_- in the interaction picture [51],

$$\begin{aligned}
\frac{d\hat{a}}{dt} &= -[i(\omega_c-\omega)+\frac{\kappa}{2}+\frac{\kappa_s}{2}]\hat{a}-g\sigma_- -\sqrt{\kappa}\hat{a}_{in},\\
\frac{d\sigma_-}{dt} &= -[i(\omega_{X^-}-\omega)+\frac{\gamma}{2}]\sigma_- -g\sigma_z\hat{a},\\
\hat{a}_{out} &= \hat{a}_{in}+\sqrt{\kappa}\hat{a},
\end{aligned} \tag{1}$$

where ω, ω_c and ω_{X^-} are the frequencies of the input probe light, cavity mode, and X^- transition, respectively. g is the coupling strength between X^- and the cavity mode, $\frac{\gamma}{2}$ and $\frac{\kappa}{2}$ are the decay rates of X^- and the cavity field, and $\frac{\kappa_s}{2}$ is the side leakage rate of the cavity.

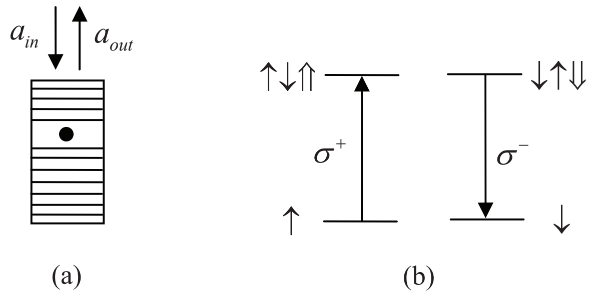

FIG. 1: The spin-dependent transitions for negatively charged exciton X^-. (a) A charged QD inside a micropillar microcavity with circular cross section. (b) Spin selection rule for optical transitions of negatively charged exciton X^- due to the Pauli's exclusion principle. σ^+ and σ^- represent a left circularly and a right circularly polarized lights, respectively.

With a weak excitation condition (X^- stays in the ground state at most time and $\langle\sigma_z\rangle=-1$), the reflection coefficient for the QD-cavity system can be obtained as follows [46],

$$r(\omega)=1-\frac{\kappa[i(\omega_{X^-}-\omega)+\frac{\gamma}{2}]}{[i(\omega_{X^-}-\omega)+\frac{\gamma}{2}][i(\omega_c-\omega)+\frac{\kappa}{2}+\frac{\kappa_s}{2}]+g^2}. \tag{2}$$

By taking $g=0$, we get the reflection coefficient for a cold cavity with the QD uncoupled to the cavity as

$$r_0(\omega)=\frac{i(\omega_c-\omega)-\frac{\kappa}{2}+\frac{\kappa_s}{2}}{i(\omega_c-\omega)+\frac{\kappa}{2}+\frac{\kappa_s}{2}}. \tag{3}$$

By adjusting the frequencies ω and ω_c, one can get $|r_0(\omega)|\cong 1$ and $|r_h(\omega)|\cong 1$. If the excess electron is in the spin state $|\uparrow\rangle$, the $|L\rangle$ light feels a hot cavity (coupled with the QD-cavity system) and gets a phase shift of φ_h after being reflected, whereas the $|R\rangle$ light feels a cold cavity and gets a phase shift of φ_0. As the linearly polarized probe beam can be regarded as the superposition of two circularly polarized components $\frac{|R\rangle+|L\rangle}{\sqrt{2}}$, the state of the reflected light becomes $e^{i\varphi_0}|R\rangle+e^{i\varphi_h}|L\rangle$ after the reflection from the one-side QD-cavity system. Conversely, if the excess electron is in the spin state $|\downarrow\rangle$, the $|L\rangle$ light feels a cold cavity and gets a phase shift of φ_0 after being reflected, while the $|R\rangle$ light feels a hot cavity and gets a phase shift of φ_h. The linear polarized probe beam $\frac{|R\rangle+|L\rangle}{\sqrt{2}}$ becomes $e^{i\varphi_h}|R\rangle+e^{i\varphi_0}|L\rangle$ after being reflected. The polarization direction of the reflected light rotates an angle $\theta_F^{\uparrow}=\frac{\varphi_0-\varphi_h}{2}=-\theta_F^{\downarrow}$, which is the so-called Faraday rotation.

If the electron is in a superposition spin state $|\psi\rangle=\alpha|\uparrow\rangle+\beta|\downarrow\rangle$ and the photon is in the state $\frac{1}{\sqrt{2}}(|R\rangle+|L\rangle)$, after being reflected, the light-spin state evolves as

$$\begin{aligned}&(|R\rangle+|L\rangle)\otimes(\alpha|\uparrow\rangle+\beta|\downarrow\rangle)\rightarrow\\&\quad e^{i\varphi_0}[\alpha(|R\rangle+e^{i\Delta\varphi}|L\rangle)|\uparrow\rangle+\beta(e^{i\Delta\varphi}|R\rangle+|L\rangle)|\downarrow\rangle],\end{aligned}\tag{4}$$

where $\Delta\varphi=\varphi_h-\varphi_0$, $\varphi_0=arg[r_0(\omega)]$, and $\varphi_h=arg[r_h(\omega)]$. In a one-side cavity, due to spin selection rule above, $|L\rangle$ and $|R\rangle$ lights pick up two different phase shifts after being reflected from the QD-cavity system, and then the state of the system composed of the light and the excess electron becomes an entangled one.

III. COMPLETE HBSA USING ONE-SIDE QD-CAVITY SYSTEMS

A hyperentangled two-photon Bell state in both the polarization and the spatial-mode DOFs has the form as

$$|\Phi^+_{AB}\rangle_{PS}=\frac{1}{2}(|RR\rangle+|LL\rangle)_{AB}\otimes(|a_1b_1\rangle+|a_2b_2\rangle)_{AB}.\tag{5}$$

Here, the subscripts A and B represent the two photons in the hyperentangled state. The subscript P denotes the polarization DOF and S is the spatial-mode DOF. a_1 (b_1) and a_2 (b_2) are the different spatial modes for the photon A (B). We denote four Bell states in the polarization DOF as

$$\begin{aligned}|\phi^\pm\rangle_P&=\frac{1}{\sqrt{2}}(|RR\rangle\pm|LL\rangle),\\|\psi^\pm\rangle_P&=\frac{1}{\sqrt{2}}(|RL\rangle\pm|LR\rangle),\end{aligned}\tag{6}$$

and four Bell states in the spatial-mode DOF as

$$\begin{aligned}|\phi^\pm\rangle_S&=\frac{1}{\sqrt{2}}(|a_1b_1\rangle\pm|a_2b_2\rangle),\\|\psi^\pm\rangle_S&=\frac{1}{\sqrt{2}}(|a_1b_2\rangle\pm|a_2b_1\rangle).\end{aligned}\tag{7}$$

Also we refer to the states $|\psi^\pm\rangle_P$ and $|\psi^\pm\rangle_S$ as the odd-parity states, and $|\phi^\pm\rangle_P$ and $|\phi^\pm\rangle_S$ as the even-parity states.

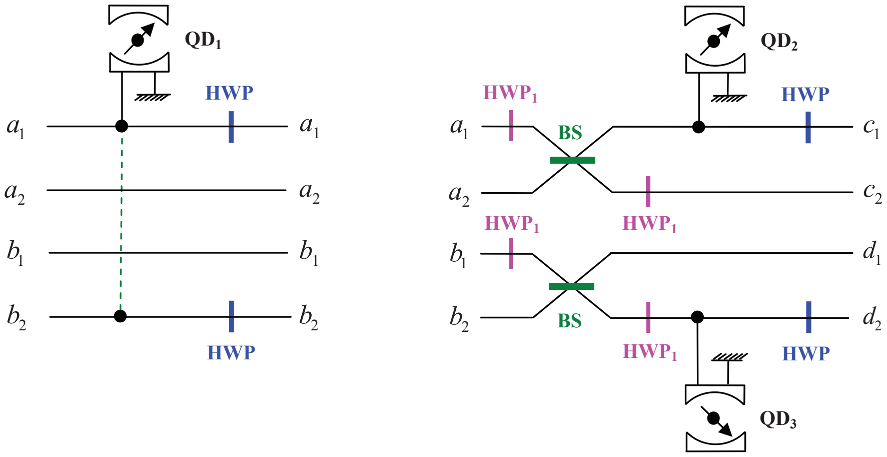

(a) (b)

FIG. 2: Schematic diagram of the present HBSA protocol for the spatial-mode entangled Bell states, without destroying the polarization Bell states of the photon pair. (a) The QND is used to distinguish the odd-parity states $|\psi^\pm\rangle_S$ from the even-parity states $|\phi^\pm\rangle_S$. (b) The QND is used to distinguish the "+" phase state $|\psi^+\rangle_S$ ($|\phi^+\rangle_S$) from the "-" phase states $|\psi^-\rangle_S$ ($|\phi^-\rangle_S$). HWP represents a half-wave plate which is used to perform a phase-flip operation $Z=|R\rangle\langle R|-|L\rangle\langle L|$ in the polarization DOF, while HWP$_1$ represents another half-wave plate which is used to perform a bit-flip operation $X=|R\rangle\langle L|+|L\rangle\langle R|$ in the polarization DOF. BS represents a 50:50 beam splitter.

A. HBSA protocol for Bell states in spatial-mode DOF

The optical properties of a singly charged QD in a strong-coupling single-side microcavity, which has been used for a controlled-phase gate, can be used to construct a quantum nondemolition detector (QND), as shown in

Fig.2. Let us assume that the initial states of the excess electron in the cavity and a single photon injected are $\frac{1}{\sqrt{2}}(|\uparrow\rangle+|\downarrow\rangle)$ and $\alpha|R\rangle+\beta|L\rangle$, respectively. By adjusting the frequencies $\omega-\omega_c \approx \frac{\kappa}{2}$ to get the phase shift difference between the left and the right circular polarization lights as $\Delta\varphi = \frac{\pi}{2}$, the function of a single photon interacting with a QD-cavity system twice is

$$\begin{aligned}&(\alpha|R\rangle + \beta|L\rangle) \otimes (|\uparrow\rangle + |\downarrow\rangle) \rightarrow \\ &\qquad e^{2i\varphi_0}(\alpha|R\rangle - \beta|L\rangle) \otimes (|\uparrow\rangle - |\downarrow\rangle).\end{aligned} \tag{8}$$

One can detect whether or not there is a photon interacted with the QD-cavity system by measuring the spin state of the excess electron with the orthogonal basis $\{|\pm\rangle = \frac{1}{\sqrt{2}}(|\uparrow\rangle \pm |\downarrow\rangle)\}$. If the excess electron is in state $|-\rangle$, there is a photon interacted with the QD-cavity system. Otherwise, there is no photon (or there are two photons) interacted with the QD-cavity system when the state of excess electron doesn't change. Therefore, if the state of excess electron in QD is not changed, there are an even number of photons detected by the QD-cavity system. With this principle, the QD-cavity system can be used as a QND to distinguish a case with an even number of photons from that with an odd number of photons.

Now, we will use this photon-number QND to construct a parity-check QND for the spatial-mode states of a photon pair. If the excess electrons in QD$_1$ in Fig.2(a) is prepared initially in the state $|+\rangle$, after the photons a and b pass through QD$_1$ in sequence, the state of the excess electron is in $|+\rangle$ with the input states $|\psi^{\pm}\rangle_S$ (odd-parity). However, the state of the excess electron becomes $|-\rangle$ if the input states are $|\phi^{\pm}\rangle_S$ (even-parity). By applying a Hadamard gate on the excess electron spin, the spin superposition states $|+\rangle$ and $|-\rangle$ can be rotated to the states $|\uparrow\rangle$ and $|\downarrow\rangle$, respectively. If we have an auxiliary photon a in the initial state $|\varphi_a\rangle = \frac{1}{\sqrt{2}}(|R\rangle + |L\rangle)$ and let it pass through QD$_1$, after it is reflected from the cavity, the state of the system composed of the photon and the QD electron spin becomes

$$\begin{aligned}(|R\rangle + |L\rangle)|\uparrow\rangle &\rightarrow e^{i\varphi_0}(|R\rangle + i|L\rangle)|\uparrow\rangle, \\ (|R\rangle + |L\rangle)|\downarrow\rangle &\rightarrow e^{i\varphi_0}(|R\rangle - i|L\rangle)|\downarrow\rangle.\end{aligned} \tag{9}$$

The output state of the auxiliary photon a can be measured in orthogonal linear polarization basis. If the auxiliary photon a is in state $|R\rangle + i|L\rangle$, the state of excess electron in QD is $|\uparrow\rangle$. Otherwise the state of excess electron in QD is $|\downarrow\rangle$. In this way, one can construct a parity-check QND for the spatial-mode states to distinguish the odd-parity states $|\psi^{\pm}\rangle_S$ from the even-parity states $|\phi^{\pm}\rangle_S$ by detecting the spin state of the excess electron in QD$_1$. The spin state of excess electron in QD$_1$ is changed for even-parity states and unchanged for odd-parity states.

With the QND in Fig.2(a), the four Bell states in the spatial-mode DOF are divided into two groups $|\psi^{\pm}\rangle_S$ and $|\phi^{\pm}\rangle_S$. The next task of BSA in spatial-mode DOF is to distinguish the different relative phases in each group. The QND shown in Fig.2(b) is used to distinguish the Bell states with the relative phase zero from those with the relative phase π. BS can accomplish the following transformation in spatial-mode DOF,

$$\begin{aligned}|a_1\rangle &\rightarrow \frac{1}{\sqrt{2}}(|c_1\rangle + |c_2\rangle), \\ |a_2\rangle &\rightarrow \frac{1}{\sqrt{2}}(|c_1\rangle - |c_2\rangle), \\ |b_1\rangle &\rightarrow \frac{1}{\sqrt{2}}(|d_1\rangle + |d_2\rangle), \\ |b_2\rangle &\rightarrow \frac{1}{\sqrt{2}}(|d_1\rangle - |d_2\rangle).\end{aligned} \tag{10}$$

After the operations by BSs in Fig.2(b), the two groups of Bell states become:

$$\begin{aligned}|\phi^+\rangle_S^{ab} &= \frac{1}{\sqrt{2}}(|a_1b_1\rangle + |a_2b_2\rangle) \rightarrow |\phi^+\rangle_S^{cd} = \frac{1}{\sqrt{2}}(|c_1d_1\rangle + |c_2d_2\rangle), \\ |\phi^-\rangle_S^{ab} &= \frac{1}{\sqrt{2}}(|a_1b_1\rangle - |a_2b_2\rangle) \rightarrow |\psi^+\rangle_S^{cd} = \frac{1}{\sqrt{2}}(|c_1d_2\rangle + |c_2d_1\rangle), \\ |\psi^+\rangle_S^{ab} &= \frac{1}{\sqrt{2}}(|a_1b_2\rangle + |a_2b_1\rangle) \rightarrow |\phi^-\rangle_S^{cd} = \frac{1}{\sqrt{2}}(|c_1d_1\rangle - |c_2d_2\rangle), \\ |\psi^-\rangle_S^{ab} &= \frac{1}{\sqrt{2}}(|a_1b_2\rangle - |a_2b_1\rangle) \rightarrow |\psi^-\rangle_S^{cd} = \frac{1}{\sqrt{2}}(|c_1d_2\rangle - |c_2d_1\rangle).\end{aligned} \tag{11}$$

That is, $|\phi^+\rangle_S^{ab}$, $|\phi^-\rangle_S^{ab}$, $|\psi^+\rangle_S^{ab}$, and $|\psi^-\rangle_S^{ab}$ become $|\phi^+\rangle_S^{cd}$, $|\psi^+\rangle_S^{cd}$, $|\phi^-\rangle_S^{cd}$, and $|\psi^-\rangle_S^{cd}$, respectively. With the parity-check measurement shown in Fig.2(b), one can read out the information about the relative phases in the groups $|\phi^{\pm}\rangle_S^{ab}$ and $|\psi^{\pm}\rangle_S^{ab}$. If the states of the excess electrons in QD$_2$ and QD$_3$ are both changed (unchanged), the state input is $|\phi^-\rangle_S^{ab}$ or $|\psi^-\rangle_S^{ab}$, and the output ports are c_1 and d_2 (c_2 and d_1). While the state of the excess electron in QD_2 is changed (unchanged) and the state of the excess electron in QD_3 is unchanged (changed), the state input is $|\phi^+\rangle_S^{ab}$ or $|\psi^+\rangle_S^{ab}$, and the output ports are c_1 and d_1 (c_2 and d_2).

The relation between the initial spatial-mode Bell states and the outcomes of the QNDs is shown in Table I. The two-photon system is in one of the two odd-parity states $|\psi^\pm\rangle_S$ in spatial-mode DOF if the state of excess electron in QD_1 is unchanged. When the state of the excess electron in QD_1 is changed, the two-photon system is in one of the two even-parity states $|\phi^\pm\rangle_S$. With QD_2 and QD_3, we read out the information about the relative phases in the groups $|\phi^\pm\rangle_S$ and $|\psi^\pm\rangle_S$. Therefore, for the state $|\psi^+\rangle_S$, the state of the excess electron in QD_1 is unchanged, and the states of the excess electrons in QD_2 and QD_3 are in combination of one changed and the other unchanged. If the state of the excess electron in QD_1 is unchanged, and the states of the excess electrons in QD_2 and QD_3 are both changed or unchanged, the input state of the two-photon system is $|\psi^-\rangle_S$. For the two-photon state $|\phi^+\rangle_S$, the state of the excess electron in QD_1 is changed, and the states of the excess electrons in QD_2 and QD_3 are in combination of one changed and the other unchanged. For the input state $|\phi^-\rangle_S$, the state of the excess electron in QD_1 is changed, and the states of the excess electrons in QD_2 and QD_3 are both changed or unchanged.

From the preceding analysis, one can see that the roles of the two QNDs are to accomplish the task of parity check. The first QND can distinguish the two even-parity states in spatial-mode DOF from the two odd-parity states. With two BSs, the two states with two different relative phases are transformed into two states with different parities. After the second QND, one can distinguish the four Bell states in spatial -mode DOF without destroying the two photons, which provides the convenience for the BSA in polarization DOF.

TABLE I: Relation between the four Bell states in the spatial-mode DOF and the output results of the measurements on electron-spin states.

Bell	Results		
States	QD_1	QD_2	QD_3
$\lvert\psi^+\rangle_S$	unchange	change (unchange)	unchange (change)
$\lvert\psi^-\rangle_S$	unchange	change (unchange)	change (unchange)
$\lvert\phi^+\rangle_S$	change	change (unchange)	unchange (change)
$\lvert\phi^-\rangle_S$	change	change (unchange)	change (unchange)

B. HBSA protocol for Bell states in polarization DOF

Now let us move our attention to distinguish the four Bell states $|\psi^\pm\rangle_P$ and $|\phi^\pm\rangle_P$ in polarization. Fig. 3 is our proposal for BSA in polarization DOF. If we sent the two photons a and b to the cavity in sequence after the BSA in spatial-mode DOF and adjust the frequencies $\omega-\omega_c \approx \frac{\kappa}{2}$ to get $\Delta\varphi = \frac{\pi}{2}$, we can get the transformation as follows.

$$\begin{aligned}(|RR\rangle \pm |LL\rangle)\otimes(|\uparrow\rangle+|\downarrow\rangle) &\rightarrow e^{2i\varphi_0}[(|RR\rangle \mp |LL\rangle)\otimes(|\uparrow\rangle-|\downarrow\rangle)],\\ (|RL\rangle \pm |LR\rangle)\otimes(|\uparrow\rangle+|\downarrow\rangle) &\rightarrow e^{i(\varphi_0+\varphi_h)}[(|RL\rangle \pm |LR\rangle)\otimes(|\uparrow\rangle+|\downarrow\rangle)].\end{aligned} \tag{12}$$

If QD_4 in Fig. 3 is prepared initially in the state $|+\rangle$, after the interaction of two photons with the QD-cavity system, one can identify whether the two-photon input states are the Bell states $|\psi^\pm\rangle_P$ (corresponding to spin $|+\rangle$) or $|\phi^\pm\rangle_P$ (corresponding to spin $|-\rangle$) by measuring the excess electron-spin state. Measuring the two photons in the polarization basis $\{|H\rangle, |V\rangle\}$, it is possible to distinguish $|\psi^+\rangle_P$ and $|\phi^+\rangle_P$ from $|\psi^-\rangle_P$ and $|\phi^-\rangle_P$, respectively. The relation between the initial Bell states in the polarization DOF and the results of the measurements on QD_4 and the two photons with the basis $\{H, V\}$ is shown in Table II.

By far, we have described the principle of our complete and deterministic HBSA with the non-linear optics in

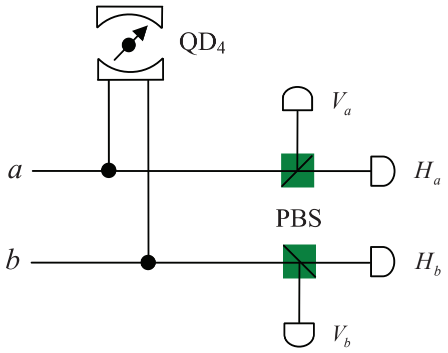

FIG. 3: Schematic diagram of the present BSA protocol for polarization Bell states. The two photons a and b are sent into the cavity in sequence.

TABLE II: The relation between the initial Bell states in the polarization DOF and the output results of the QD$_4$ and the single-photon detections.

Bell	Results	
States	QD$_4$	Detector
$\vert\psi^+\rangle_P$	unchange	$\{H_a, H_b\}$ or $\{V_b, V_b\}$
$\vert\psi^-\rangle_P$	unchange	$\{H_a, V_b\}$ or $\{V_a, H_b\}$
$\vert\phi^+\rangle_P$	change	$\{H_a, V_b\}$ or $\{V_a, H_b\}$
$\vert\phi^-\rangle_P$	change	$\{H_a, H_b\}$ or $\{V_a, V_b\}$

one-side QD-cavity systems. The BSA on the spatial and the polarization-mode DOFs can be realized by adjusting the frequencies $\omega - \omega_c \approx \frac{\kappa}{2}$ to get the phase shift $\Delta\varphi = \frac{\pi}{2}$.

IV. APPLICATIONS OF HBSA IN QUANTUM COMMUNICATION

As a complete and deterministic analysis on quantum states is important in quantum communication, it is interesting to discuss the applications of HBSA. Let us use hyperentanglement swapping as an example to describe its principle.

Hyperentanglement swapping enables two parties in quantum communication to obtain hyperentanglement between two particles which do not interact with each other initially. Suppose that the two entangled pairs AB and CD are in the following hyperentangled states:

$$|\Phi^+\rangle_{AB} = \frac{1}{2}(|RR\rangle + |LL\rangle)_{AB} \otimes (|a_1 b_1\rangle + |a_2 b_2\rangle)_{AB},$$
$$|\Phi^+\rangle_{CD} = \frac{1}{2}(|RR\rangle + |LL\rangle)_{CD} \otimes (|c_1 d_1\rangle + |c_2 d_2\rangle)_{CD} \tag{13}$$

The subscripts A and B denote that the particles are in nodes A and B, respectively, as shown in Fig. 4. Alice shares a photon pair AB with Bob, and she also shares a photon pair CD with Charlie. The task of this hyperentanglement-swapping protocol is to entangle the two photons A and D in both the polarization and the spatial-mode DOFs.

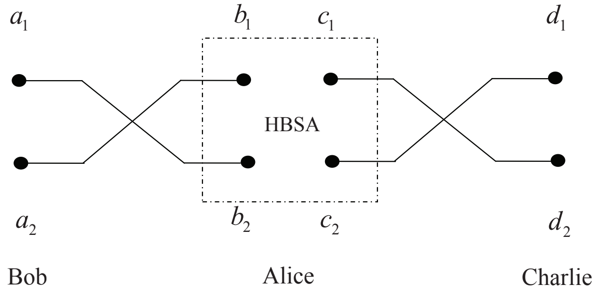

FIG. 4: Schematic diagram for the hyperentanglement swapping in both the polarization and the spatial-mode DOFs. The initial hyperentangled states are prepared in nodes AB and CD (also the four photons). After Alice performs the HBSA on the two photons BC, Bob and Charlie can get the hyperentangled state between nodes A and D.

To complete entanglement swapping of hyperentangled states, Alice performs HBSA on the two particles B and C in her hand, as shown in Fig. 4. The state of the whole system can be rewritten as

$$\begin{aligned}|\Phi^+\rangle_{AB} \otimes |\Phi^+\rangle_{CD} \;=\; & \frac{1}{4}[(|\phi^+\rangle_P^{AD}|\phi^+\rangle_P^{BC} + |\phi^-\rangle_P^{AD}|\phi^-\rangle_P^{BC} + |\psi^+\rangle_P^{AD}|\psi^+\rangle_P^{BC} + |\psi^-\rangle_P^{AD}|\psi^-\rangle_P^{BC}) \\ & \otimes(|\phi^+\rangle_S^{AD}|\phi^+\rangle_S^{BC} + |\phi^-\rangle_S^{AD}|\phi^-\rangle_S^{BC} + |\psi^+\rangle_S^{AD}|\psi^+\rangle_S^{BC} + |\psi^-\rangle_S^{AD}|\psi^-\rangle_S^{BC})].\end{aligned} \tag{14}$$

If the outcome of HBSA is $|\phi^+\rangle_P^{BC}|\phi^+\rangle_S^{BC}$, the two photons located in the nodes A and D is in the hyperentangled state $|\phi^+\rangle_P^{AD}|\phi^+\rangle_S^{AD}$. The other outcomes lead to the other hyperentangled states, such as $|\phi^+\rangle_P^{AD}|\phi^-\rangle_S^{AD}$, $|\phi^-\rangle_P^{AD}|\phi^\pm\rangle_S^{AD}$, $|\phi^\pm\rangle_P^{AD}|\psi^\pm\rangle_S^{AD}$, $|\psi^\pm\rangle_P^{AD}|\phi^\pm\rangle_S^{AD}$, and $|\psi^\pm\rangle_P^{AD}|\psi^\pm\rangle_S^{AD}$. In principle, it is not difficult for Bob and Charlie to transform their hyperentangled state into the form $|\phi^+\rangle_P^{AD}|\phi^+\rangle_S^{AD}$. For instance, if Bob and Charlie obtain the state $|\psi^-\rangle_P^{AD}|\psi^-\rangle_S^{AD}$, the state $|\phi^+\rangle_P^{AD}|\phi^+\rangle_S^{AD}$ can be obtained in the way that Charlie performs an operation $-\sigma_y = |R\rangle\langle L| - |L\rangle\langle R|$ in polarization (both the two spatial modes d_1 and d_2) and then exchanges the two spatial modes after he introduces a phase π in the spatial mode d_1 with a $\frac{\lambda}{2}$ wave plate.

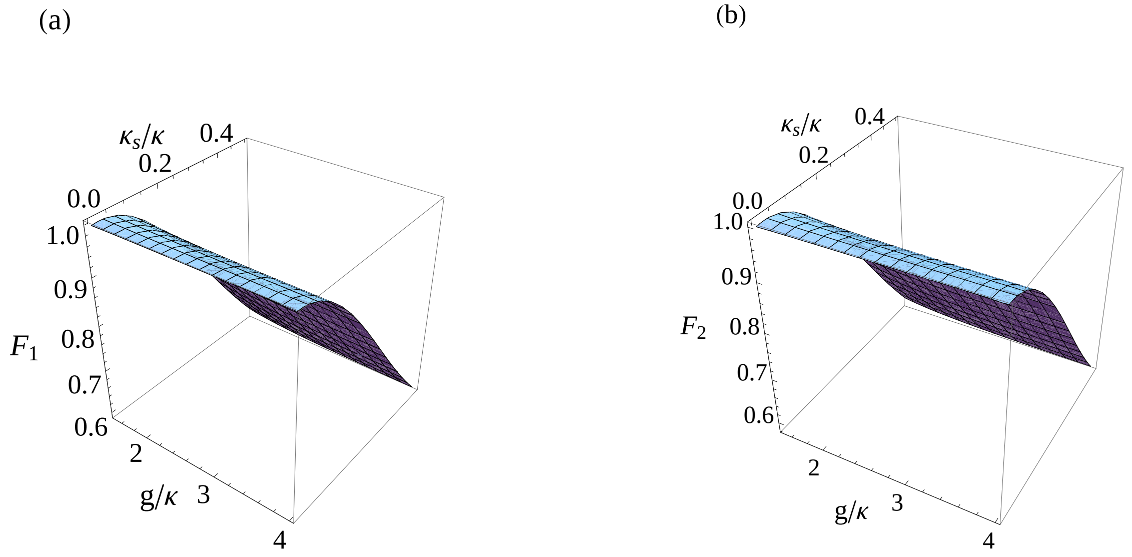

FIG. 5: Fidelity of the present HBSA vs the coupling strength for different side leakage rates with $\gamma = 0.1\kappa$. (a) Fidelity of the HBSA for these hyperentangled Bell states with the spatial-mode state $|\phi^-\rangle_S$. (b) Fidelity of the HBSA for these hyperentangled Bell states with the spatial-mode state $|\phi^+\rangle_S$.

The hyperentanglement-swapping protocol presented here is completed by two simultaneous but independent processes, including both the polarization BSA and the spatial-mode BSA. If we only perform the Bell-state measurement on the photons B and C in the polarization DOF, photons A and D will be entangled in the polarization degree of freedom but leave their state in the spatial-mode DOF be a mixed one.

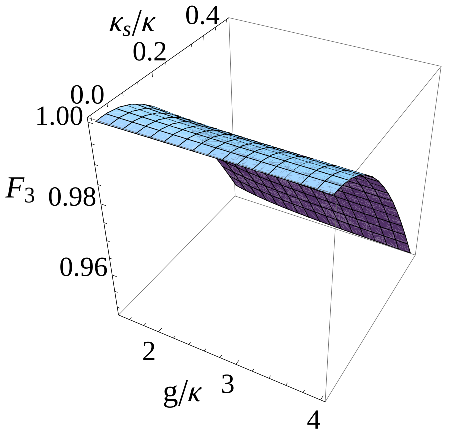

FIG. 6: Fidelity of the process for detecting the excess electron in QD vs the coupling strength for different side leakage rates with $\gamma = 0.1\kappa$.

V. DISCUSSION AND CONCLUSION

BSA is essential in quantum communication, especially in long-distance quantum communication assisted by quantum repeater. There are many proposals for analyzing Bell states in polarization photon pairs. For the hyperentangled BSA discussed here, the entanglements in different DOFs need to be analyzed independently. This is different from the hyperentanglement-assisted BSA in polarization DOF, in which other degree of freedom is used as an additional system and is consumed in the analysis.

In our proposal, the BSA in the polarization and the spatial-mode DOFs are completed by the relative phase shift $\frac{\pi}{2}$ of left circularly and right circularly polarized lights . In 2011, Young et al. [52] showed that a QD-induced phase shift of 0.2 rad between an (effectively) empty cavity and a cavity with a resonantly coupled QD can be deduced, by using a single-photon level probe. With improved mode matching and pillar design, this phase shift could be much larger. If the cavity side leakage is neglected, the fidelity of the proposed proposal can reach 100% in the strong-coupling regime with $|r_0(\omega)| \cong 1$ and $|r_h(\omega)| \cong 1$. However, there is rigorous limitation in the QD-micropillar cavity. Defining fidelity as $F = |\langle\psi_f|\psi\rangle|^2$, the fidelities for hyperentangled Bell states with the spatial-mode state $|\phi^-\rangle_S$ is,

$$F_1=\frac{(|r_0|^2+|r_h|^2)^4}{8(|r_0|^4+|r_h|^4)^2}+\frac{[(|r_0|^4-|r_h|^4)^2+4|r_h|^2|r_0|^2(|r_h|^2+|r_0|^2)^2]^2}{32[(|r_0|^8-|r_h|^8)^2+4|r_h|^4|r_0|^4(|r_h|^4+|r_0|^4)^2]}, \tag{15}$$

and the fidelities of hyperentangled Bell states with spatial-mode state $|\phi^+\rangle_S$ is

$$F_2=\frac{[|r_0|^6+|r_h|^6+3|r_0|^2|r_h|^2(|r_0|^2+|r_h|^2)]^2}{8[|r_0|^{12}+|r_h|^{12}+3|r_0|^4|r_h|^4(|r_0|^4+|r_h|^4)]}. \tag{16}$$

Here $|\psi_f\rangle$ is the final state of the total system which includes the external reservoirs, and $|\psi\rangle$ is the final state with an ideal condition. From these two functions, one can see that different spatial modes of input hyperentangled Bell states will interact with QD-cavity systems for different times. If the input hyperentangled Bell states have the spatial modes in an even parity, only one photon interacts with the QD-cavity system. While the input hyperentangled Bell states with the spatial modes in an odd parity, two photons may both interact with the QD-cavity system or both do not interact with the QD-cavity system. Fig. 5 is the fidelities of hyperentangled Bell states with the spatial modes in $|\phi^-\rangle_S$ and $|\phi^+\rangle_S$. The detection of the excess electron in QD requires auxiliary photon interacting with the QD-cavity system, and the fidelity of this process is

$$F_3=\frac{1}{2}+\frac{1}{\frac{|r_0|}{|r_h|}+\frac{|r_h|}{|r_0|}}. \tag{17}$$

Fig. 6 is the fidelity of process for detecting the excess electron. In these figures, the fidelities are ultimately limited by the cavity leakage, which results in a not-unity reflectance and reduces the success probability of the whole analysis process. If the cavity side leakage can be controlled, the fidelity of QD-cavity system may be higher.

In summary, we have proposed a complete HBSA scheme with the interaction between a circular polarization light and an one-side QD-cavity system. We use the relative phase shift of the right and the left circular lights to construct parity-check measurements and analyze Bell states in different DOFs of photon paris. We also discussed its applications in long-distance quantum communication processes in two different DOFs simultaneously.

ACKNOWLEDGEMENTS

This work is supported by the National Natural Science Foundation of China under Grant Nos. 10974020 and 11174039, NCET-11-0031, and the Fundamental Research Funds for the Central Universities.

[1] A. K. Ekert, Phys. Rev. Lett. **67**, 661 (1991).
[2] C. H. Bennett, G. Brassard, and N. D. Mermin, Phys. Rev. Lett. **68**, 557 (1992).
[3] N. Gisin, G. Ribordy, W. Tittel, and H. Zbinden, Rev. Mod. Phys. **74**, 145 (2002).
[4] G. L. Long and X. S. Liu, Phys. Rev. A **65**, 032302 (2002).
[5] F. G. Deng and G. L. Long, Phys. Rev. A **68**, 042315 (2003).
[6] C. H. Bennett and S. J. Wiesner, Phys. Rev. Lett. **69**, 2881 (1992).
[7] X. S. Liu, G. L. Long, D. M. Tong, and F. Li, Phys. Rev. A **65**, 022304 (2002).
[8] C. H. Bennett, G. Brassard, C. Crépeau, R. Jozsa, A. Peres, and W. K. Wootters, Phys. Rev. Lett. **70** , 1895 (1993).
[9] M. Żukowski, A. Zeilinger, M. A. Horne, and A. K. Ekert, Phys. Rev. Lett. **71**, 4287 (1993).
[10] L. Vaidman and N. Yoran, Phys. Rev. A **59**, 116 (1999).
[11] N. Lütkenhaus, J. Calsamiglia, and K. A. Suominen, Phys. Rev. A **59**, 3295 (1999).
[12] J. Calsamiglia, Phys. Rev. A **65**, 030301(R) (2002).
[13] K. Mattle, H. Weinfurter, P. G. Kwiat, and A. Zeilinger, Phys. Rev. Lett. **76**, 4656 (1996).
[14] J. A. W. van Houwelingen, N. Brunner, A. Beveratos, H. Zbinden, and N. Gisin, Phys. Rev. Lett. **96**, 130502 (2006).
[15] R. Ursin, T. Jennewein, M. Aspelmeyer, R. Kaltenbaek, M. Lindenthal, P. Walther, and A. Zeilinger, Nature (London) **430**, 849 (2004).
[16] Z. Y. Ou and L. Mandel, Phys. Rev. Lett. **61**, 50 (1988).
[17] Y. H. Shih and C. O. Alley, Phys. Rev. Lett. **61**, 2921 (1988).
[18] J. G. Rarity and P. R. Tapster, Phys. Rev. Lett. **64**, 2495 (1990).
[19] A. Mair, A. Vaziri, G. Weihs, and A. Zeilinger, Nature (London) **412**, 313 (2001).
[20] N. K. Langford, R. B. Dalton, M. D. Harvey, J. L. O'Brien, G. J. Pryde, A. Gilchrist, S. D. Bartlett, and A. G. White, Phys. Rev. Lett. **93**, 053601 (2004).
[21] J. D. Franson, Phys. Rev. Lett. **62**, 2205 (1989).
[22] J. Brendel, N. Gisin, W. Tittel, and H. Zbinden, Phys. Rev. Lett. **82**, 2594 (1999).
[23] D. V. Strekalov, T. B. Pittman, A. V. Sergienko, and Y. H. Shih, Phys. Rev. A **54**, R1 (1996).
[24] T. Yang, Q. Zhang, J. Zhang, J. Yin, Z. Zhao, M. Żukowski, Z. B. Chen, and J. W. Pan, Phys. Rev. Lett. **95**, 240406 (2005)
[25] C. Cinelli, M. Barbieri, R. Perris, P. Mataloni, and F. De Martini, Phys. Rev. Lett. **95**, 240405 (2005).

[26] J. T. Barreiro, N. K. Langford, N. A. Peters, and P. G. Kwiat, Phys. Rev. Lett. **95**, 260501 (2005).
[27] M. Barbieri, C. Cinelli, P. Mataloni, and F. De Martini, Phys. Rev. A **72**, 052110 (2005).
[28] G. Vallone, R. Ceccarelli, F. De Martini, and P. Mataloni, Phys. Rev. A **79**, 030301(R) (2009).
[29] P. G. Kwiat and H. Weinfurter, Phys. Rev. A **58**, 2623(R) (1998).
[30] S. P. Walborn, S. Ṕadua, and C. H. Monken, Phys. Rev. A **68**, 042313 (2003).
[31] C. Schuck, G. Huber, C. Kurtsiefer, and H. Weinfurter, Phys. Rev. Lett. **96**, 190501 (2006).
[32] M. Barbieri, G. Vallone, P. Mataloni, and F. De Martini, Phys. Rev. A **75**, 042317 (2007).
[33] J. T. Barreiro, T. C. Wei, and P. G. Kwiat, Nature. Phys **4**, 282 (2008).
[34] T. C. Wei, J. T. Barreiro, and P. G. Kwiat, Phys. Rev. A **75**, 060305(R) (2007).
[35] C. Simon and J. W. Pan, Phys. Rev. Lett. **89**, 257901 (2002).
[36] Y. B. Sheng, F. G. Deng, and H. Y. Zhou, Phys. Rev. A **77**, 042308 (2008).
[37] Y. B. Sheng and F. G. Deng, Phys. Rev. A **81**, 032307 (2010).
[38] Y. B. Sheng and F. G. Deng, Phys. Rev. A **82**, 044305 (2010).
[39] X. H. Li, Phys. Rev. A **82**, 044304 (2010).
[40] F. G. Deng, Phys. Rev. A **83**, 062316 (2011).
[41] Y. B. Sheng and F. G. Deng, Phys. Rev. A **81**, 042332 (2010).
[42] Y. B. Sheng, F. G. Deng, and G. L. Long, Phys. Rev. A **82**, 032318 (2010).
[43] P. Kok, W. J. Munro, K. Nemoto, T. C. Ralph, J. P. Dowling, and G. J. Milburn, Rev. Mod. Phys. **79**, 135 (2007).
[44] J. H. Shapiro, Phys. Rev. A **73**, 062305 (2006).
[45] J. Gea-Banacloche, Phys. Rev. A **81**, 043823 (2010).
[46] C. Y. Hu, A. Young, J. L. O'Brien, W. J. Munro, and J. G. Rarity, Phys. Rev. B **78**, 085307 (2008).
[47] C. Y. Hu, W. J. Munro, and J. G. Rarity, Phys. Rev. B **78**, 125318 (2008).
[48] C. Y. Hu and J. G. Rarity, Phys. Rev. B **83**, 115303 (2011).
[49] R. J. Warburton, C. S. Dürr, K. Karrai, J. P. Kotthaus, G. Medeiros-Ribeiro, and P. M. Petroff, Phys. Rev. Lett. **79**, 5282 (1997).
[50] C. Y. Hu, W. Ossau, D. R. Yakovlev, G. Landwehr, T. Wojtowicz, G. Karczewski, and J. Kossut, Phys. Rev. B **58**, R1766 (1998).
[51] D. F. Walls and G. J. Milburn, *Quantum Optics*, Springer-Verlag, Berlin, (1994).
[52] A. B. Young, R. Oulton, C. Y. Hu, A. C. T. Thijssen, C. Schneider, S. Reitzenstein, M. Kamp, S. Höfling, L. Worschech, A. Forchel, and J. G. Rarity, Phys. Rev. A **84**, 011803 (2011).